Journal of Materials Chemistry

Cite this: J. Mater. Chem., 2012, 22, 1054

www.rsc.org/materials

PAPER

Photocurable polymer gate dielectrics for cylindrical organic field-effect transistors with high bending stability†

Jaeyoung Jang,[ab] Sooji Nam,[ab] Jihun Hwang,[b] Jong-Jin Park,*[a] Jungkyun Im,[a] Chan Eon Park*[ab] and Jong Min Kim*[a]

Received 22nd August 2011, Accepted 18th October 2011
DOI: 10.1039/c1jm14091d

Here we describe the use of photocurable poly(vinyl cinnamate) (PVCN) as a gate dielectric in high-performance cylindrical organic field-effect transistors (OFETs) with high bending stability. A smooth-surface metallic fiber (Al wire) was employed as a cylindrical substrate, and polymer dielectrics (PVCN and poly(4-vinyl phenol) (PVP)) were formed *via* dip-coating. The PVCN and PVP dielectrics deposited on the Al wire and respectively cross-linked *via* UV irradiation and thermal heating were found to be very smooth and uniform over the entire coated area. Pentacene-based cylindrical OFETs with the polymer dielectrics exhibited high-performance hysteresis-free operation. Devices made with the PVCN dielectric showed superior bending stability than devices made with PVP dielectrics or previously reported cylindrical OFETs due to the good flexibility of the PVCN dielectric. The devices maintained their excellent performance under bending at a bending radius comparable to the lowest value reported for planar OFETs.

1. Introduction

Organic semiconductors and polymer dielectrics have attracted considerable recent interest for use in low-cost flexible electronic devices, such as organic field-effect transistors (OFETs).[1–3] Their unique electronic and mechanical properties enable the preparation of functional OFETs on cylindrical fiber-shaped substrates, which are a key component of the newly emerging field of electronic textiles (e-textiles) geared toward development of wearable electronics.[4–12] The market for e-textiles is continuously growing. Major electronics and materials companies have developed various types of e-textiles such as medical shirts monitoring the patient's vital signs and fabric-based military sensors identifying the enemy's approach.[4] However, these prototypes reported thus far have been fabricated by attaching conventional electric components directly onto clothes.[5,6] Ultimately, the electronic components should be integrated into a fiber itself and mass-production manufacturing schemes *via* weaving the electronic functional fiber are required.[5–7] Recently, cylindrical fiber-shaped OFETs embedded in textiles (tulle or silk) and their woven logic devices were reported.[5–7] Although mechanical stress-durability will be a critical issue in such devices for everyday wear, the fabrication of cylindrical OFETs with high bending stability still remains a challenge.[4] Nevertheless, research on improving the performance and stability of cylindrical OFETs has been scarce because OFET fabrication on cylindrical substrates is more difficult than on planar substrates (*i.e.*, wafer, glass, or plastic substrates).[8,11]

Two main approaches have been used in the preparation of cylindrical OFETs: (1) fabrication of transistors at the intersection of two fibers,[5–7] and (2) fabrication of a device on a single fiber substrate.[8–10] The former devices were demonstrated by creating junctions using an electrolyte gate dielectric lump between two fibers. Although this type of transistor has many advantages, the devices may be susceptible to mechanical bending stress that dislocates the two functional fibers, resulting in deformation of the transistors. OFETs on a single fiber substrate were fabricated using vacuum-deposited oxide dielectrics[8] or polymer dielectrics[9,10] and pentacene as a semiconductor. However, these devices showed poor bending stress durability[8,10] and electrical performance[8,9] compared with planar OFETs having the same device configuration, probably due to the rough surface of the metallic fiber substrates. A rough surface decreases the electrical strength of a gate dielectric by increasing the effective electric field,[13] and disturbs formation of a uniform smooth gate dielectric layer as well as formation of a highly crystalline organic semiconductor layer on the gate dielectric.[14]

Here, we demonstrate the preparation of high-performance cylindrical OFETs using two types of cross-linkable insulating polymers as the gate dielectrics, the thermally or

[a]*Samsung Advanced Institute of Technology (SAIT), Yongin, 449-712, Republic of Korea. E-mail: cep@postech.ac.kr; jongjin00.park@samsung.com; jongkim@samsung.com*
[b]*POSTECH Organic Electronics Laboratory, Polymer Research Institute, Department of Chemical Engineering, Pohang University of Science and Technology, Pohang, 790-784, Korea*

† Electronic supplementary information (ESI) available. See DOI: 10.1039/c1jm14091d

photochemically cross-linkable polymers, poly(vinyl phenol) (PVP) and poly(vinyl cinnamate) (PVCN), respectively. As shown in the schematic device diagram in Fig. 1(a), a metallic fiber (Al wire) was employed as a cylindrical gate substrate with a low surface roughness prepared by electropolishing. The polymer dielectrics were formed by dip-coating and the effect of the surface roughness on the formation of the polymer dielectrics was systematically investigated. Studies of dip-coated polymer dielectrics on cylindrical substrates have been sparse,[10] although dip-coating is the most appropriate coating method among solution-processing techniques (such as spin-coating, drop-casting, and printing techniques). Uniform, smooth, and cross-linked PVP and PVCN gate dielectrics were used to prepare pentacene-based cylindrical OFETs, and the devices were submitted to bending experiments. Although both devices exhibited high-performance hysteresis-free operation, OFETs with PVCN gate dielectrics showed much better bending stress durability than OFETs with PVP gate dielectrics because of the good flexibility of PVCN. The minimum bending radius (R_{min}) of PVCN devices was comparable to the lowest value reported for planar OFETs. Our study provides an understanding of the effects of the polymer gate dielectrics and their processing conditions on the performance and mechanical stress durability of OFETs with a cylindrical geometry.

2. Experimental

Sample preparation

A PVP solution was prepared by dissolving PVP (Aldrich, M_w = 23 000) and a cross-linker, poly(melamine-*co*-formaldehyde) methylated (PMF, Aldrich), in a 3 : 1 weight ratio in tetrahydrofuran (Aldrich, anhydrous), resulting in a total solution concentration of 0.175 g g^{-1}. A PVCN solution was prepared by dissolving PVCN (Aldrich, M_w = 230 000) in chloroform (Aldrich, anhydrous) in a solution concentration of 0.039 g g^{-1}. The chemical structures of PVCN and PVP are shown in Fig. 1

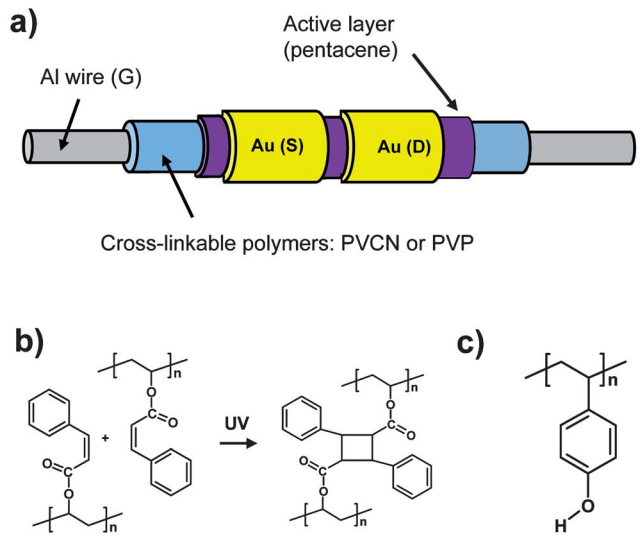

Fig. 1 (a) Schematic device structure of the cylindrical OFETs used in this study. (b) The chemical structures of PVCN (left), photo-chemically cross-linked PVCN (right), and PVP (c).

(b) and (c), respectively. An Al wire substrate (Aldrich, radius was measured to be 350 μm using calipers) was electropolished at a constant voltage of 20 V in a mixture solution containing perchloric acid (60%) : ethanol in a volume ratio of 1 : 4 at a constant temperature of 7 °C for 5–20 min using a cylinder-shaped carbon electrode (see Fig. S1†).[15] After rinsing with DI water, the wire substrate was dipped into the PVP or PVCN polymer solution at a constant rate of 1000 μm s^{-1} then lifted out at a constant rate of 100 μm s^{-1}. The PVP coated wire was then placed in a vacuum oven and cured at 200 °C for 1 h to produce cross-linking, as shown in the chemical reaction presented in Fig. S2†.[16] The PVCN was photocured through the chemical reaction presented in Fig. 1(b) by UV light illumination (λ = 255 nm, power = 50 W) (G15T8, Sankyo Denki) of the PVCN-coated wire for 20 min. The wire was rotated to achieve a uniform curing rate.[17] All steps (solution preparation and coating) using PVCN were performed in the dark under ambient conditions. Fifty-nanometre thick active layers of pentacene were deposited through a shadow mask on the gate dielectrics at a rate of 0.2 Å s^{-1} using an organic molecular beam deposition system. Gold source/drain electrodes were deposited by thermal evaporation through a shadow mask onto the active layer. Because the pentacene and gold electrodes were deposited without rotating the substrate wire, the layers covered about half of the wire.[9] The channel width (W) was calculated to be $\pi \times R$ (~1100 μm), and the channel length (L) was 150 μm.

Characterization

An atomic force microscope (AFM, Multimode SPM, Digital Instruments), a scanning electron microscope (SEM, S-4800, Hitachi), and a confocal microscope (λ = 408 nm, OLS 3000, Olympus) were used to characterize the surface morphologies of the polymers and pentacene layers. Tilted-view SEM images of the device cross-section were characterized by imaging a device cross-section after focused ion beam (FIB) (FIB2200, Seiko) milling of the OFET fabricated on the Al wire substrate. The conditions for milling were 30 kV for the I-beam, and side view images were collected with a typical positive slope of 52°. An HP 4284A Precision LCR meter (Agilent Tech.) was used to measure the capacitance per unit area (C_i). All electrical characteristics of the OFETs were measured under ambient conditions (RH: 40 (±15)%) using Keithley 2400 and 236 source/measure units. The field-effect mobility (μ) was obtained from the slope of a plot of the square-root of the drain current ($I_D^{1/2}$) against the gate voltage (V_G), using the equation $I_D = \mu C_i(W/2L)(V_G - V_{Th})^2$, where V_{Th} is the threshold voltage. In the bending experiments, the electrical characteristics of the devices were measured in a bent state imposed by bending the devices over one of the three half-round glass tubes, as shown in Fig. S3†. As the strain increased, the C_i value of the bilayer gate dielectric increased slightly, and the values of μ were calculated to reflect the changes in C_i.

3. Results and discussion

Because metal wires (including the Al wires used in this study) have extremely rough surfaces, they must be smoothed prior to use as an OFET substrate. Fig. S1† shows time-dependent SEM

images of the Al wire as a function of the electropolishing time. The surface of the Al wire gradually smoothed up to 10 min of polishing time, and polishing beyond 10 min produced a rough surface. The wires prepared by various electropolishing times were dip-coated into PVP or PVCN solutions as schematized in Fig. 2(b), and the effects of the surface roughness on the formation of polymer gate dielectrics were investigated. The polymer gate dielectric films were examined using confocal microscopy with pointwise illumination (λ = 408 nm), which provides high optical resolution and contrast relative to conventional optical microscopy using wide-field illumination.[18] Confocal microscopy images of the dip-coated PVP and PVCN prepared on the Al wires electropolished for various times are shown in Fig. S4†. Although the polymer films revealed similar morphologies, determined by wide-field optical microscopy (data not shown), the confocal microscopy images of the polymer films displayed different degrees of surface roughness. The polymer films coated on the un-polished bare wires could not fill the deepest pockets of the wire surface, and the surface was not smooth after application of the polymer coating. The flexure of the polymer films coated on the polished wires became more moderate as the polishing time increased from 5 to 10 min. Note that the wavelength used for confocal microscopy was 408 nm, which means that the interference patterns (bright and shaded areas) produced by height differences in the film were sensitive to length scales of 1/4 λ, 102 nm. The Al wire polished for 10 min produced the most uniform polymer films, and was used as the cylindrical substrate in all subsequent experiments. Fig. 2(a) shows the schematic illustration of the polymer-coated wire, and Fig. 2(c)–(f) illustrate typical confocal microscopy images for the initial point and midpoint of the dip-coated PVP and PVCN films on a polished wire, respectively. As illustrated in Fig. 2(c) and (e), PVP and PVCN films showed 5-fold and 4-fold interference patterns, which implied film thicknesses of approximately 1020 (5/2 of λ) and 816 nm (4/2 of λ), respectively. The midpoints of the dip-coated polymer films were uniform (according to the confocal microscopy images) and smooth (according to the AFM images of PVP and PVCN in Fig. 2(g) and (h), respectively). The r.m.s. roughness (R_q) of PVP and PVCN films was 0.311 and 0.323 nm, respectively, within the 5 × 5 μm^2 scan area. This roughness was comparable to that of spin-coated polymer films on planar glass or wafer substrates.[17,19]

The thickness and uniformity of the polymer film were examined by fabricating Al wire/polymer/Au metal–insulator–metal (MIM) capacitors and investigating the cross-section of the gold top electrodes. Fig. 3(a) and (b) show tilted-view SEM images of a cross-section after FIB milling of the MIM capacitors fabricated on Al wire substrates, with PVP and PVCN films, respectively. Each gold or polymer layer was clearly resolved, and the thicknesses of PVP and PVCN films were 650 and 500 nm, respectively. These values were lower than the values inferred by the confocal microscopy images of the polymer films shown in Fig. 2(c) and (e), which suggests that the films were thicker at the initial point than at the midpoint of the substrate. The uniformity of the coated films over the entire wire substrate was assessed by measuring the capacitances of the 6 MIM capacitors located at positions along a single wire, as indicated in the schematic diagram in the inset of Fig. 3(d). Because the capacitance of a MIM capacitor was proportional only to the thickness of the insulator for an insulating material (that is, the relative permittivity (k) was fixed), the distribution of capacitance measurements provides a good index for the thickness

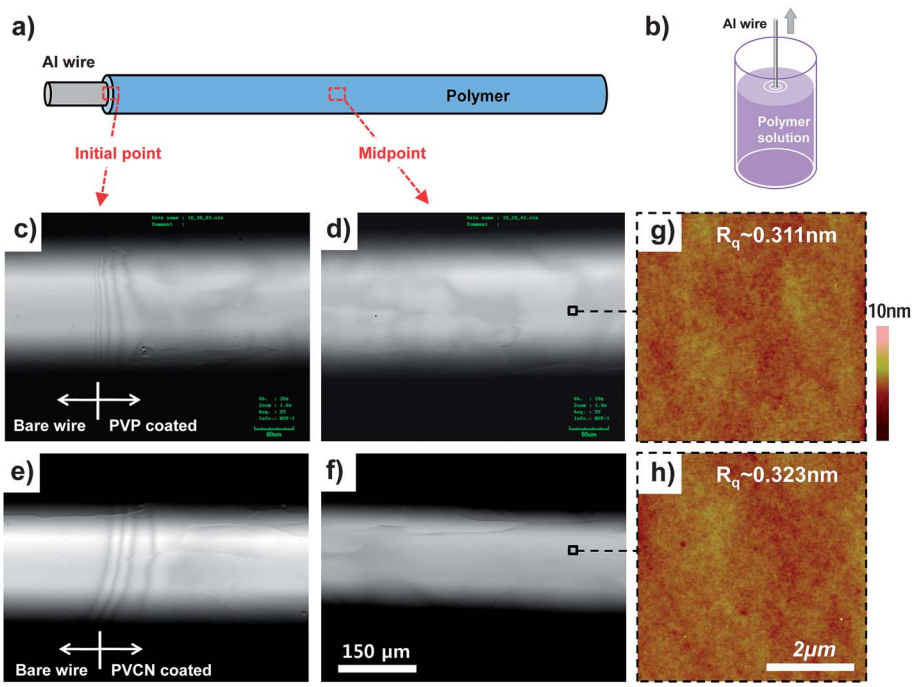

Fig. 2 (a) A schematic illustration of a polymer-coated Al wire and (b) the dip-coating process. Confocal microscopy images of dip-coated PVP at an initial point (c) and midpoint (d), and PVCN at an initial point (e) and midpoint (f). Height-mode AFM topographs of PVP (g) and PVCN (h) gate dielectrics.

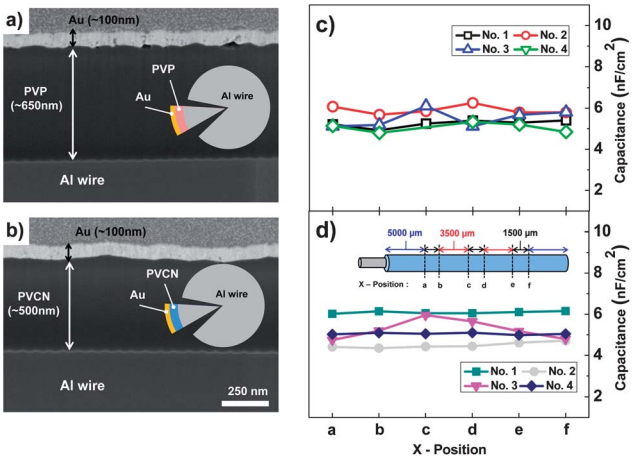

Fig. 3 Tilted-view SEM images of cross-sections taken after FIB milling of the MIM capacitors incorporating PVP (a) and PVCN (b) dielectrics. The inset images show a schematic illustration of the device cross-section. The C_i values of MIM capacitors using PVP (c) and PVCN (d) dielectrics as a function of the x-position. The inset of (d) illustrates a schematic representation of the x-position of 6 MIM capacitor devices in a polymer-coated wire.

uniformity of the polymer films coated on the wire. The relationship among C_i, k, permittivity of free space (ε_0), and film thickness (t) is given as follows: $C_i = k\varepsilon_0/t$. Fig. 3(a) and (b) show the capacitance values of 4 wire samples as a function of the MIM capacitor x-position for PVP and PVCN, respectively. Although the capacitance values differed slightly among the 4 wires at a given x-position, the values were almost constant at all x-positions within a single wire.

Fig. 4(a) and (b) show the optical microscopy device top-view images of the OFETs using a pentacene semiconductor layer and gold source/drain electrodes deposited on the PVP and PVCN gate dielectrics, respectively, on Al wires. Typical dendritic

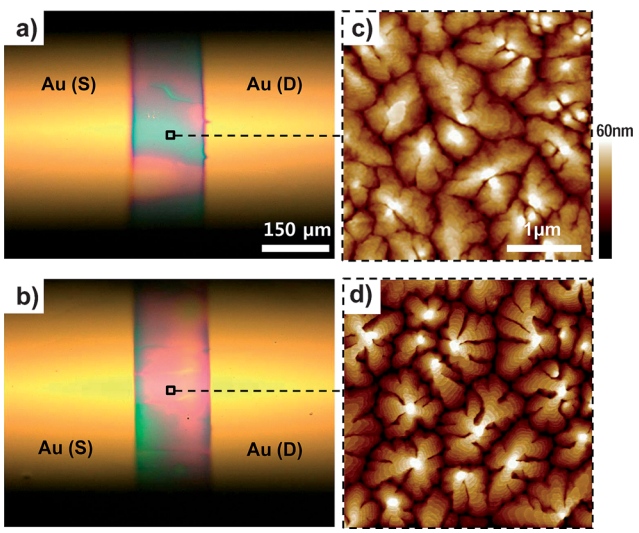

Fig. 4 Device top-view optical microscopy images of the cylindrical OFETs prepared using PVP (a) and PVCN (b) dielectrics. Height-mode AFM topographs of the pentacene thin films on PVP (c) and PVCN (d) dielectrics.

pentacene grains of average size 1 μm were observed in the AFM images at positions where the pentacene layers were clearly resolved, as shown in Fig. 4(c) (PVP) and Fig. 4(d) (PVCN). The morphologies and size of the pentacene grains were similar to those of the reported pentacene layers grown on PVP and PVCN gate dielectrics coated on smooth and planar wafers or glass substrates.[17,19] Fig. 5(a) and (b) show typical V_G *versus* I_G, $I_D^{1/2}$, and I_D transfer characteristics in the saturation regime with dual V_G sweeps for the cylindrical pentacene OFETs using dip-coated PVP and PVCN gate dielectrics, respectively. Both OFETs exhibited high-performance hysteresis-free operation with a low leakage current, suggesting that both the PVP and PVCN gate dielectrics were well-deposited (without pinholes) *via* dip-coating, and the polymers were well-cross-linked. The average transistor properties are summarized in Table 1 (total of 12 OFETs (3 OFETs in a batch, 4 batches in total) were tested, and the OFET parameters were averaged). Typical drain voltage (V_D) *versus* I_D output characteristics of both OFETs are shown in Fig. 5(c) and (d), exhibiting good linear/saturation behavior.

The effects of bending strain on the performance of the cylindrical OFETs incorporating the polymer gate dielectrics were measured. Three types of half-round glass tubes with different diameters (see Fig. S3†) were used to apply a constant tensile strain during an electrical measurement, as illustrated in the inset of Fig. 6(d). Fig. 6(a) and (b) show the transfer characteristics as a function of the bending radius (R), and Fig. 6(c) and (d) show the relationship between R and μ and between R and V_{Th} for the cylindrical OFETs using PVP and PVCN gate dielectrics, respectively. As presented in Fig. 6, the OFETs with PVCN dielectric exhibited excellent stability against the applied tensile strain, whereas the OFETs with PVP dielectric exhibited poor stability. Although the OFETs with PVP dielectric showed better bending stability than the reported cylindrical OFETs in

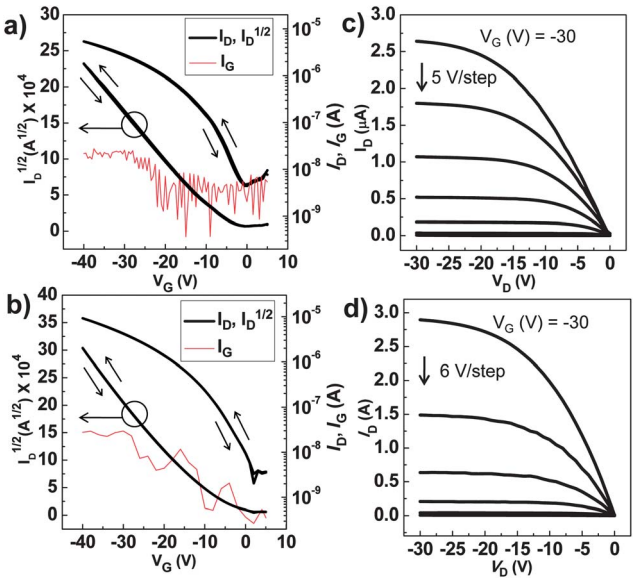

Fig. 5 Typical V_G *versus* I_G, I_D, and $I_D^{1/2}$ transfer characteristics (in dual V_G sweeps) of the cylindrical OFETs incorporating PVP (a) and PVCN (b) gate dielectrics. Typical I_D *versus* V_D output characteristics of the cylindrical OFETs incorporating PVP (c) and PVCN (d) gate dielectrics (V_D and $V_G = -40$ V).

Table 1 Transistor parameters for pentacene-based cylindrical OFETs using PVP and PVCN gate dielectrics (V_D and $V_G = -40$ V)

OFETs dielectric	C_i/nF cm^{-2}	μ/cm^2 V^{-1} s^{-1}	V_{Th}/V	On–off ratio
Thermally cross-linked PVP	5.0	0.24 (±0.04)	−4.78 (±0.09)	2.53×10^3
Photo-cross-linked PVCN	5.12	0.53 (±0.03)	−7.05 (±0.06)	4.21×10^3

the literature,[8,10] considering that the PVP-based devices still work under the applied strain of $R \approx 2.2$, the μ and V_{Th} values of the PVP-based device were not stably maintained as the strain increased. Moreover, the devices failed to function under high-strain conditions of $R \approx 1.0$. On the other hand, OFETs using PVCN dielectrics retained their high performance, even under an applied strain of $R \approx 1.0$. The values of μ remained above 85% of their unstrained value, and V_{Th} decreased from their unstrained levels by only 0.9% with bending. As summarized in Table 2, the OFET performance under the R_{min} tested here was superior to any performance under bending strain previously reported for cylindrical OFETs.[8,10] The performance of the PVCN-based OFETs under bending strain was comparable to the lowest reported result for planar OFETs[20] without a thick polymer encapsulation layer used to create a strain-neutral position.[2,21] (Here, we considered OFETs with μ exceeding 0.1 cm^2 V^{-1} s^{-1}, and defined the R_{min} as the lowest value of R that retained a μ exceeding 85% of the unstrained value.)

Two main reasons can explain the superior strain durability of the PVCN-based OFETs compared with PVP-based OFETs. First, thermally cross-linked PVP may be more rigid and stiffer than photochemically cross-linked PVCN because the degree of cross-linking in PVP may be higher than in PVCN. In general, it is difficult to fully cross-link a photocrosslinkable polymer simply using photoirradiation because the molecular motion of the polymer chains decreases as the molecular weight increases upon cross-linking.[22,23] On the other hand, high-temperature heating increases polymer chain motion during cross-linking, thereby increasing the degree of cross-linking, which makes the films more rigid. The amount of hysteresis in the transfer curves for OFETs prepared using PVP dielectrics provides a good index for the degree of cross-linking because the amount of hysteresis is generally proportional to the amount of residual hydroxyl groups in a polymer dielectric.[24,25] Lee *et al.* recently reported that pentacene OFETs with PVP dielectrics showed negligible hysteresis if the PVP was fully cross-linked using an optimized cross-linking process.[25] Our cylindrical pentacene OFETs prepared with PVP dielectrics also showed negligible hysteresis during operation under ambient conditions, suggesting a high degree of cross-linking in the PVP dielectrics. The degree of

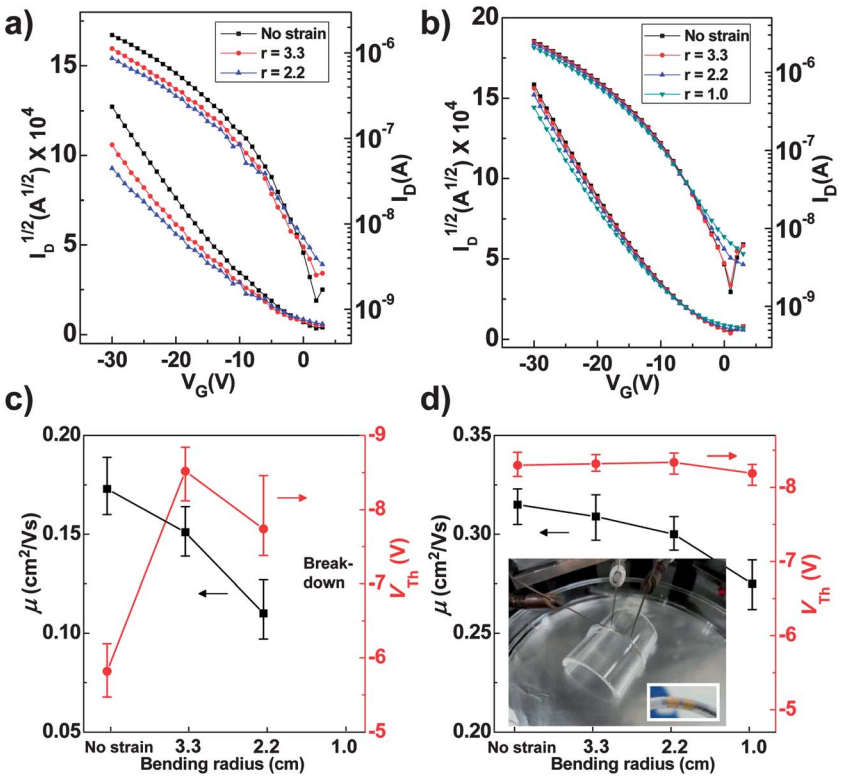

Fig. 6 V_G *versus* I_D, and $I_D^{1/2}$ transfer characteristics of cylindrical OFETs using PVP (a) and PVCN (b) gate dielectrics as a function of R. Variations in μ and V_{Th} of the devices prepared using PVP (c) or PVCN (d) gate dielectrics as a function of R (V_D and $V_G = -30$ V). The inset digital camera image of (d) illustrates a cylindrical wire involving 4 OFET devices in a bent state during electrical measurements and a single OFET device in a bent state (inset).

Table 2 Comparison of the charge carrier mobility and R_{min} with the literature values. Here, we consider OFETs with μ exceeding 0.1 $cm^2 V^{-1} s^{-1}$, and we define the R_{min} as the lowest value of R for which μ exceeds 85% of their unstrained value

Parameters	Cylindrical OFETs w/ SiO_2 gate dielectrics (ref. 8)	Cylindrical OFETs w/PVP gate dielectrics (ref. 10)	Planar OFETs w/PVP gate dielectrics (ref. 20)	Cylindrical OFETs w/PVCN gate dielectrics (this work)
$\mu/cm^2 V^{-1} s^{-1}$	0.02	0.50	0.41	0.53
R_{min}	8	8	0.55	1.0

cross-linking is not expected to be proportional to the amount of hysteresis for the PVCN-based OFETs because PVCN is a hydroxyl group-free polymer. Devices prepared using PVCN dielectrics mostly exhibit hysteresis-free operations.[17,23] Second, the main chain of PVCN may be more flexible than that of PVP. This is because, in general, the elongation at break of the vinyl polymers whose side group is connected with polymer backbone by the ester group is much higher than that of the vinyl polymers whose side group is connected by the phenyl group. For example, the elongation at break values of poly(vinyl acetate) and poly (methyl methacrylate) are respectively 10–20% and 4–5.5%, which are about 3–10 times higher than that of polystyrene, 1.5% (see Fig. S5† for their chemical structures).[26] The rotation about C–O–C bonds has low energy barrier, and therefore the side group connected with polymer backbone by the ester group is much more flexible than the side group connected by the rigid phenyl group.[27]

To support our speculation, we measured C_i values for MIM capacitors of the PVP and PVCN dielectrics as a function of the applied tensile strain. As shown in Fig. S6†, the relative C_i increased by 1.028 upon bending for the photo-cured PVCN gate dielectrics. On the other hand, the relative C_i could not increase by above 1.014 for thermally cross-linked PVP dielectrics and, at higher strain, the dielectrics eventually showed electrical breakdown (*i.e.* the devices short-circuited). As mentioned above, the measured C_i provides information of the average thickness of the film underlying the gold electrode of a MIM capacitor, on the assumption that $k\varepsilon_0$ is constant. In other words, the relative film thickness to the initial value of the photo-cured PVCN gate dielectrics is lower than that of the thermally cross-linked PVP dielectrics under the maximum applied strain. These results imply that the photo-cured PVCN gate dielectrics can stretch more than the thermally cross-linked PVP dielectrics and that the photo-cured PVCN dielectrics exhibit better elongation property than the thermally cross-linked PVP dielectrics. Our work presents that the pentacene-based cylindrical OFETs using PVCN dielectrics showed outstanding bending strain durability due to the extremely smooth Al wire substrate, the uniform deposition of the polymer dielectrics on the wire, and the flexible mechanical properties/chemical nature of the photocurable PVCN.

4. Conclusions

In summary, we demonstrate high-performance pentacene-based cylindrical OFETs using dip-coated cross-linkable polymers, PVP and PVCN, as the gate dielectrics. An Al wire was employed as a cylindrical substrate, the surface of which was smoothed by a 10 min electropolishing process. The polymer dielectrics formed on the substrate showed smooth surface characteristics, uniform film morphologies, and strong insulating properties. Cylindrical OFETs prepared with either PVP or PVCN gate dielectrics yielded high-performance operation without hysteresis. Bending experiments revealed that the cylindrical OFETs prepared using PVCN gate dielectrics exhibited remarkably higher bending stress durability than the OFETs prepared using PVP gate dielectrics, due to the better flexibility of the photocurable PVCN dielectrics. The devices prepared with PVCN gate dielectrics retained their high performance under the applied tensile strain, in which the bending radius was comparable to the minimum value reported for planar OFETs.

Acknowledgements

This work was supported by a grant from the Korea Science and Engineering Foundation (KOSEF) and National Research Foundation of Korea as a part of Global Frontier Research Center for Advanced Soft Electronics, funded by the Korea government (MEST) (20110000330). J. Jang and S. Nam contributed equally to this work.

References

1 C. D. Dimitrakopoulos and P. R. L. Malenfant, *Adv. Mater.*, 2002, **14**, 99.
2 D. Braga and G. Horowitz, *Adv. Mater.*, 2009, **21**, 1473.
3 T. Sekitani, U. Zschieschang, H. Klauk and T. Someya, *Nat. Mater.*, 2010, **9**, 1015.
4 R. F. Service, *Science*, 2003, **301**, 909.
5 M. Hamedi, R. Forchheimer and O. Inganäs, *Nat. Mater.*, 2007, **6**, 357.
6 M. Hamedi, L. Herlogsson, X. Crispin, R. Marcilla, M. Berggren and O. Inganäs, *Adv. Mater.*, 2009, **21**, 573.
7 C. Müller, M. Hamedi, R. Karlsson, R. Jansson, R. Marcilla, M. Hedhammar and O. Inganäs, *Adv. Mater.*, 2011, **23**, 898.
8 J. B. Lee and V. Subramanian, *IEEE Int. Electron Devices Meet.*, 2003, 8.3.1–8.3.4.
9 M. Maccioni, E. Orgiu, P. Cosseddu, S. Locci and A. Bonfiglio, *Appl. Phys. Lett.*, 2006, **89**, 143515.
10 J. B. Lee and V. Subramanian, *IEEE Trans. Electron Devices*, 2005, **52**, 269.
11 J. Liu, M. A. G. Namboothiry and D. L. Carroll, *Appl. Phys. Lett.*, 2007, **90**, 063501.
12 B. O'Connor, K. H. An, Y. Zhao, K. P. Pipe and M. Shtein, *Adv. Mater.*, 2007, **19**, 3897.
13 Y.-P. Zhao, G.-C. Wang and T.-M. Lu, *Phys. Rev. B: Condens. Matter Mater. Phys.*, 1999, **60**, 9157.
14 P. S. Jo, J. Sung, C. Park, E. Kim, D. Y. Ryu, S. Pyo, H.-C. Kim and J. M. Hong, *Adv. Funct. Mater.*, 2008, **18**, 1202.
15 C. Yang, K. Shin, S. Y. Yang, H. Jeon, D. Choi, D. S. Chung and C. E. Park, *Appl. Phys. Lett.*, 2006, **89**, 153508.
16 S. H. Kim, S. Nam, J. Jang, K. Hong, C. Yang, D. S. Chung, C. E. Park and W.-S. Choi, *J. Appl. Phys.*, 2009, **105**, 104509.
17 J. Jang, S. H. Kim, S. Nam, D. S. Chung, C. Yang, W. M. Yun, C. E. Park and J. B. Koo, *Appl. Phys. Lett.*, 2008, **92**, 143306.
18 J. A. Lim, W. H. Lee, H. S. Lee, J. H. Lee, Y. D. Park and K. Cho, *Adv. Funct. Mater.*, 2008, **18**, 229.

19 T.-W. Lee, J. H. Shin, I.-N. Kang and S. Y. Lee, *Adv. Mater.*, 2007, **19**, 2702.
20 A. Jedaa and M. Halik, *Appl. Phys. Lett.*, 2009, **95**, 103309.
21 T. Sekitani, S. Iba, Y. Kato, Y. Noguchi, T. Someya and T. Sakurai, *Appl. Phys. Lett.*, 2005, **87**, 173502.
22 K. S. Anseth, L. M. Kline, T. A. Walker, K. J. Anderson and C. N. Bowman, *Macromolecules*, 1995, **28**, 2491.
23 J. Jang, S. H. Kim, J. Hwang, S. Nam, C. Yang, D. S. Chung and C. E. Park, *Appl. Phys. Lett.*, 2009, **95**, 073302.
24 S. Lee, B. Koo, J. Shin, E. Lee, H. Park and H. Kim, *Appl. Phys. Lett.*, 2006, **88**, 162109.
25 S. C. Lim, S. H. Kim, J. B. Koo, J. H. Lee, C. H. Ku, Y. S. Yang and T. Zyung, *Appl. Phys. Lett.*, 2007, **90**, 173512.
26 J. Brandrup, E. H. Immergut and E. A. Grulke, *Polymer Handbook*, John Wiley & Sons, 4th edn, 1999, vol. 1, ch. 5, pp. 78, 87 and 166.
27 C. Tosi, *Theor. Chim. Acta*, 1982, **62**, 29.

